Ductile fractures and magma migration from source

Roberto F. Weinberg[1] and Klaus Regenauer-Lieb[2]
[1]School of Geosciences, Monash University, Clayton, Victoria 3800, Australia
[2]School of Earth and Geographical Sciences, The University of Western Australia, Perth, Western Australia 6009, Australia, and Commonwealth Scientific and Industrial Research Organisation (CSIRO) Exploration & Mining, Kensington, Western Australia 6151, Australia

ABSTRACT

Mechanisms proposed to explain efficient melt transport away from hot, ductile source regions are problematic. Brittle-elastic fracturing is a well-known mechanism that allows fast magma migration as dikes through cold crust. Ductile fractures have been propo sed as an alternative for ductile environments, where brittle-elastic diking is inhibited. Ductile fracturing results from rock creep and growth of microscale voids that become interconnected, leading to rock failure. In this paper, we present observations and numerical models supporting the hypothesis that ductile fracture controls early steps in magma migration. We postulate that once developed, ductile fracture dikes may reach a critical length where magma stresses at dike tips overcome fracture toughness and lead to brittle-elastic diking, which subsequently controls magma migration.

INTRODUCTION

The issue of magma transport from hot and ductile anatectic source to upper crust has generally been approached by simplifying rock behavior to either a viscoelastic or a brittle-elastic material. This has led to vigorous debate (Petford et al., 2000) about whether magmas rise as diapirs (Weinberg and Podladchikov, 1994); as porosity waves (Connolly and Podladchikov, 1998); or as dikes (Lister and Kerr, 1991). Diking allows fast magma transfer and may generate a self-organized network of fractures and a permeable magma pathway (Bons and van Milligen, 2001; Brown, 2004; Petford and Koenders, 1998). However, dike initiation processes remain unclear (Rubin, 1998).

Diking refers to the brittle-elastic process of open-mode fracturing (mode I) driven by magma, and propagation normal to the direction of minimum compression (Pollard and Segall, 1987). Stresses are magnified at dike tips, and propagation occurs when tip stresses equate to fracture toughness (Lister and Kerr, 1991; Rubin, 1998), or when reduced stresses lead to subcritical crack growth (Chen and Jin, 2006). Fracture toughness studies suggest a change in failure mechanism from brittle to ductile mode II shear conjugates as temperature increases (Gandhi and Ashby, 1979). Laboratory (Hirth and Tullis, 1994) and field analyses (Stockhert et al., 1999) on natural quartzites suggest that the transition temperature is as low as ~300 °C. Thus, the high pressure-temperature (*P-T*) conditions typical of anatectic regions inhibit the elastic mechanisms that drive brittle-elastic diking (Weinberg, 1999). Volume increase due to partial melting may lead to melt-enhanced embrittlement (Rushmer, 1995); however, the micromechanisms underlying this process can range from brittle to ductile fracturing (Gandhi and Ashby, 1979). Several mechanisms have been proposed (Bons and van Milligen, 2001; Brown, 2004; Petford and Koenders, 1998), but there is a lack of agreement on a mechanism that satisfactorily explains speed, volumes, and geometries of magma transfer through ductile rocks (Petford et al., 2000; Rubin et al., 2005; Stracke et al., 2006).

Ductile fracturing tends to initially follow mode II shear bands (Thomason, 1989). This mechanism is now being considered in the geosciences (Eichhubl, 2004; Eichhubl and Aydin, 2003; Regenauer-Lieb, 1999) to explain features of strongly deformed brittle-ductile rocks (Dimanov et al., 2007; Rybacki et al., 2008; Shigematsu et al., 2004), and failure of melt-bearing rocks (Brown, 2004; Závada et al., 2007). Here, we investigate whether ductile fracturing controls melt migration. We describe the process of ductile fracturing and the applied numerical methodology used to investigate the process. We then present features of an interconnected dike network exposed in the Pangong Range, NW India, to compare with numerical model results.

DUCTILE FRACTURING

Ductile or creep fracture is well-known in metallurgy and ceramics. This mechanism is characterized by crystal plasticity or creep, which are time-dependent processes, unlike brittle-elastic fracturing. Ductile fracture relies on various mechanisms that cause "microstructural damage" (Rogers, 1979). There are different classes of ductile fracture (Thomason, 1989). Here, we provide a generic description common to all classes.

Ductile fracturing is divided into three stages (Fig. 1; Gandhi and Ashby, 1979). In the first stage, deformation is controlled by creep through dislocation accompanied by small elastic dilation in the vicinity of dislocation walls. In the second stage, microstructural dilation sets in. The micromechanics of ductile microvoid nucleation rely on shear displacement on microstructural heterogeneities (e.g., rigid/soft inclusion, dislocation pile-up on grain boundary) or on shear displacements as grain-boundary sliding, leading to net opening at a grain triple junction. At this stage, various mechanisms lead to strain localization into shear zones. This dilation has significantly larger magnitude than elastic dilation and is a result of microvoid nucleation and growth by microbrittle or microductile (creep) processes. These processes are usually a function of grain size and take place either at grain contacts (decohesion) or by failure across larger particles. Preferential growth of microvoids in the center of shear zones leads to the formation of "void sheets" (Fig. 1). In the third stage, plastic instability of the matrix between microvoids leads to void-void coalescence and ductile fracturing. While stages 1 and 2 happen at creeping strain rates, rupture in stage 3 can be much faster. The entire three-stage process constitutes ductile fracturing. In geological systems, at depths larger than a few kilometers, microvoids would be filled with either fluids or melts.

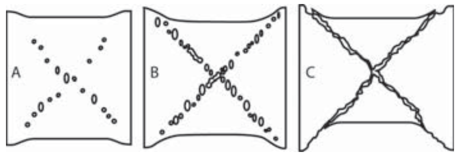

Figure 1. Evolution of conjugate set of ductile fractures in pure shear horizontal extension (after Shigematsu et al., 2004). A–B: Microstructural dilation stage 2 with increasing void density in center of shear zones, accompanied by grain-size reduction. C: Void-void coalescence leading to ductile fracture (stage 3).

METHODS

We modeled numerically an initial two-dimensional (2-D) rectangular block, of 100 × 100 finite elements, 50 m high and 100 m wide. The block is extended horizontally in pure shear at a constant velocity of 6 mm/yr applied to the left and right boundaries (12 mm/yr in total). Deformation is plane strain, and the top and bottom boundaries are free to move. The temperature is 923 K, and in order to avoid brittle behavior, pressure is equivalent ~8 kbar, and the rheology is that of wet quartz (Hirth et al., 2001). For the given boundary conditions and flow laws, the numerical results produce relatively fast strain rates, ensuring that the deformation creep regime is restricted to that of power-law creep (dislocation), excluding other ductile fracture mechanisms caused by dislocation glide, diffusion creep, or cleavage. Different patterns would emerge for experiments at lower temperatures or lower velocities, where brittle behavior or diffusion, respectively, might dominate (see Gandhi and Ashby, 1979). Very low-strength melt pods the size of one element are randomly distributed in the model.

In the calculations, pore nucleation rate and growth in the presence of fluids are a function of strain rate and bulk strain. We used the simplest empirical Gurson formulation (Tvergaard and Needleman, 1992) for stage 3, which does not consider the active role of melt, such as melt-accelerated necking and void interaction. This implies that ductile fractures grow in the models without additional acceleration related to melt pressure or void-void coalescence, as in more sophisticated models (Tvergaard and Needleman, 1992). Thus, magmas move passively into ductile fractures.

Ductile fracturing has been the subject of intense studies in theoretical and applied mechanics. We use here the most widely used approach to model the degradation of materials due to continuum damage caused by ductile microvoid nucleation and coalescence. The approach is based on describing a population of microvoids generated through ductile shearing inside a representative volume element, RVE, in terms of a "smeared crack." A plastic potential is used as a continuum representation taking into account material degradation caused by both microvoid nucleation and growth. The microvoid pore space volume fraction becomes a damage state variable that is tracked for each RVE (for details, see Regenauer-Lieb, 1999).

The void volume ratio, f, is defined by $f = 1 - r$, where r is the solid rock density divided by the actual density of the rock. Dynamic void evolution is described by $\dot{f} = \dot{f}_{nuc} + \dot{f}_{gr}$ where the growth rate is controlled by the mass conservation, $\dot{f}_{gr} = \dot{\varepsilon}\,(1 - f)$, and the nucleation rate is assumed to be strain-rate controlled, $\dot{f}_{nuc} = A\dot{\varepsilon}^h$, where the superscript h stands for hardening, and

$$A = \frac{f_N}{\sqrt{2\pi} \bullet s_N} \exp\left[-\frac{1}{2}\left(\frac{\varepsilon^h - \varepsilon_N}{s_N}\right)^2\right]$$

defines a normal distribution of void volume fraction f_N nucleating around the nucleation strain, ε_N, with the standard deviation s_N. In our calculations, $\varepsilon_N = 30\%$, and voids nucleate with a void volume fraction f_N of 4% of the total volume. These scaling values are derived from experiments on metals (Needleman and Tvergaard, 1992). The empirical approach of Gurson is limited by lack of data for rocks. We therefore used empirical data for metals, which provide a conservative lower limit for fracture initiation in materials with capacity for brittle cleavage, such as rocks and ceramics. This implies that we only allow for crack growth and nucleation through crystal plastic creep processes and neglect the possibility of brittle microcracking, as well as brittle crack growth around melt inclusions. Therefore, the nucleation strain in rocks is expected to be lower than ε_N <30%, and the population densities of melt inclusions inside the solid matrix have f_N >4%. Once pores are nucleated, they can grow or contract depending on whether deformation is dilational or contractional, respectively. Linkage between pores is achieved by pore growth and by the weakening effect of pores on the rheology (Gurson criterion; Regenauer-Lieb, 1999). The higher is the concentration of pores, the more they weaken the surrounding, thus increasing pore growth rates in a runaway process that ends in pore linkage and catastrophic failure (Rybacki et al., 2008). In the models, the influence of pores on rock strength is implemented through a cosine hyperbolic function in stress space (Regenauer-Lieb, 1999). Equations were solved using Abaqus v. 6.7.

Simplifying assumptions were made when applying results from metallurgy and ceramics to rock deformation. In Earth's crust, the existence of overlying rocks prevents access of atmospheric gas to the microvoids. We assumed that microvoids are filled with melts or aqueous fluids. Each void is not a separate entity, but voids are treated as a population in a given finite element. For this population, we assumed that the pressure integral of the void-filling melt relaxes to that of the surrounding solid matrix. Since microvoids are initially small and background strain rate is slow, this assumption is unlikely to be violated in stages 1 and 2 of ductile fracturing. However, it is likely to be violated during the accelerated phase of failure (stage 3). We also assume that void-filling melt has negligible viscosity. This is justified on the basis that deformation is controlled by the strong matrix, and there is negligible melt flow. Again, this assumption breaks down in stage 3, when a connected melt sheet forms, and the solid matrix ceases to control melt behavior. Thus, our numerical models simulate the dynamics of stages 1 and 2, but not of stage 3 because of the important role of melt flow.

In the calculation, thermal diffusion is considered while chemical diffusion processes are neglected. Thermal perturbations produced through shear heating around initial melt inclusions propagate rapidly through the model because of the small length scale considered. In order to maintain a conservative limit for the initiation of ductile fractures, other positive feedback processes, such as chemical feedback or thermal expansion, are not considered. Strain localization is entirely due to ductile fracturing. Given this numerical setup, the results are scale independent between 1 km and the size of the element, as long as this is significantly larger than grain size. At scales larger than 1 km, shear heating is likely to play an important role. At small scales, grain size is one of the factors controlling the population density of microcracks, which in turn controls ductile fracturing (see Regenauer-Lieb, 1999).

DIKE NETWORK IN PANGONG RANGE

The Pangong Range in northwest India exposes a dike network with a number of peculiar features (Table 1; Fig. 2). The rock sequence consists of calk-alkaline intrusions into amphibolites interlayered with psammites,

TABLE 1. DISTINGUISHING FEATURES BETWEEN DUCTILE FRACTURE AND BRITTLE-ELASTIC DIKES; SKETCH DEPICTS DUCTILE FRACTURE DIKES FEEDING BRITTLE-ELASTIC DIKES

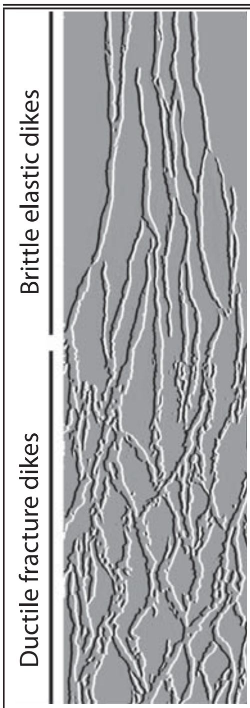

Ductile fracture dikes	Brittle-elastic dikes
Mode II: conjugate sets, irregular orientations	Mode I: single set normal to tensile stress axis
Shear zone association rarely preserved	No association with shear zone
Blunt tips	Sharp tips
Dikes merge, no crosscutting contacts or offsets	Common crosscutting of multiple dike sets
Tortuous margins, zigzagging trends	Straight margins
High-T surroundings at time of intrusion	Low-T surroundings at time of intrusion

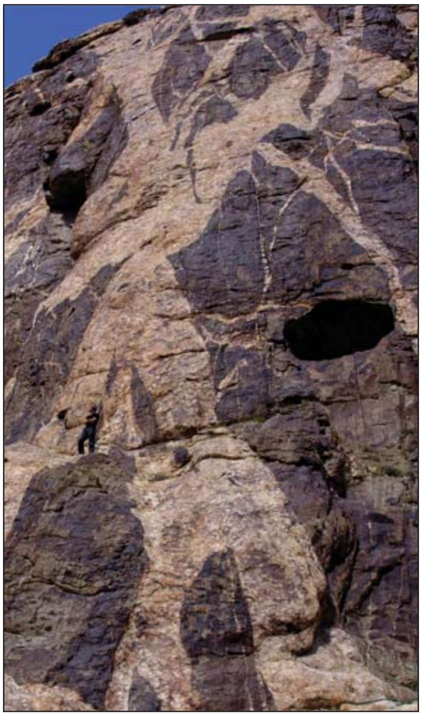

Figure 2. Dike network in calc-silicate layer in Pangong Range, NW India (34°08′38″N, 78°08′12″E). Looking northwest approximately down plunge of dike intersection, plane exposed is perpendicular to bedding. Note lack of mutual dike truncation and displacement of intersecting dikes.

pelites, and a layered calc-silicate sequence up to hundreds of meters wide. Calc-alkaline intermediate rocks, biotite amphibolites, and psammites underwent water-present partial melting at 17–15 Ma, forming migmatites and leucogranite sheets (Weinberg and Mark, 2008). Pressure and temperature during melting, and by inference during magma intrusion, are estimated to be ~700–750 °C and ~4–5 kbar (Rolland and Pêcher, 2001).

Calc-silicate rocks did not undergo anatexis but were intruded by a network of leucogranite dikes compositionally and mineralogically identical to those found in surrounding migmatites, and interpreted to be derived from these. Dikes vary in width from 0.01 to 10 m and form an anastomosing network (Fig. 2), isolating locally rotated blocks of calc-silicate rock. Dike attitudes were measured in accessible outcrops with three-dimensional (3-D) exposure, but not in two-dimensional (2-D) subvertical outcrops like in Figure 2.

While migmatites surrounding the calc-silicate layer record upright folding and a steep foliation indicative of horizontal shortening during transpressive shearing associated with the Karakoram shear zone (Weinberg and Mark, 2008), the calc-silicate layer was extended horizontally to accommodate magma intrusion. This difference in behavior was probably related to volume changes through magma transfer from the surrounding anatectic rocks out of the system. Reconstruction of calc-silicate fragments in Figure 2 indicates a near-horizontal extension of ~36% and a near-vertical extension of ~15% (see Fig. DR1 in the GSA Data Repository[1]).

Dikes form a continuous anastomosing network, with few dangling dike tips exposed (Fig. 2). They are tortuous and vary in width over relatively short distances. The most striking feature of the network is the absence of dike truncation or mutual offsets. Rather, at close range, magmatic rocks form a single continuous body. Dikes define a common intersection plunging moderately northwest (329/38), which is interpreted to represent the intermediate stress axis at intrusion (Fig. DR2). Two dike orientations can be defined in Figure 2 with an average acute angle of 67° ± 15°, measured in the 2-D surface, in a plane close to normal to the plunge of their intersection. They are interpreted to have intruded along conjugate planes of maximum shear stress dipping north and southwest and are roughly bisected by the subvertical plane parallel to bedding (Fig. 2).

NUMERICAL MODELS

In the numerical models, a ductile fracture network arises with a well-defined conjugate set of fractures after ~10,000 yr of deformation (Figs. 3A–3B). Fractures develop at small bulk shear strains (2% to 3%; Fig. 3A) coincident with regions of void growth. Fractures zigzag in an irregular pattern, have sharp boundaries, and lack mutual offsets (Fig. 3A). At the late stage shown, two main fractures remain active (Fig. 3B). They merge to form a Y shape (base of Fig. 3B), and a small block is captured and rotated in between the fractures.

A characteristic of ductile fracture is that pores nucleate only in regions where pressures are lower than lithostatic. These pressures arise out of applied external forces interacting with random perturbations. Pore nucleation amplifies the negative pressure gradient through further dilation, thereby attracting fluids into the pores. Once pores start to coalesce into a macroscopic ductile fracture (stage 3), the model registers a peak of pressure drop followed by recovery to background pressure. This process would give rise to ductile fracture dikes.

DISCUSSION

Unlike brittle-elastic dikes, ductile fracture dikes exploit mode II fractures, which are temporally related to high-temperature deformation, produce a zigzag geometry, and have blunt tips (Table 1; Brown, 2004). Another distinguishing feature is the absence of lateral displacement or crosscutting relationships (Fig. 2).

Ductile fracturing is typically preceded by ductile shearing. However, neither the model nor the natural example records visible shearing along fracture margins. This is because fracturing obliterates the shear pattern, and ductile fractures require only modest local shear straining (2% to 3%; Fig. 3A) to reach stage 3. This strong sensitivity of fracturing to void nucleation is probably underestimated in the models because: (1) the Tvergaard accelerated pore growth model enhances ductile fracture (Regenauer-Lieb, 1999); (2) models use the high value for the strain controlling pore nucleation from metals (statistically void nucleation peaks at 30% strain), whereas ceramics are better rock analogues, and void nucleation in these peaks at ~14% strain (Knott, 1973); and (3) other positive feedback mechanisms, such as chemical, thermal expansion, and diffusion or dislocation glide feedbacks, are not considered. Thus, it is likely that ductile fracturing in rocks with a small fluid/melt fraction occurs after only modest shearing, and evidence for shearing is unlikely to be preserved. However, diagnostic strain gradients may be preserved in the absence of a fluid phase, which would delay ductile fracture initiation (Rybacki et al., 2008) and induce large prefracture strain

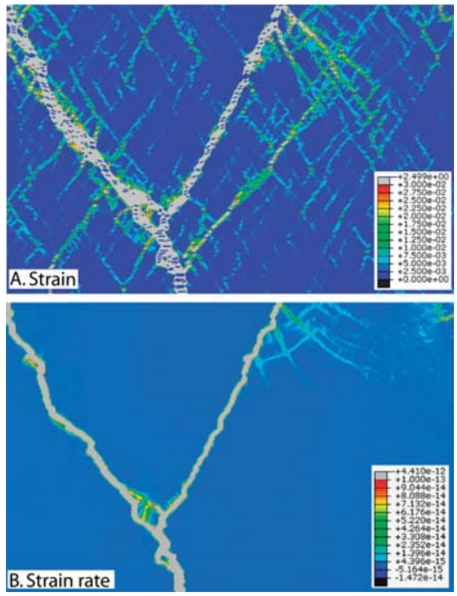

Figure 3. Results of numerical model of ductile fracturing after 41 k.y. A: Bulk strain. Fractures define conjugate sets with local variations. Note variety in orientations. B: Strain rate (s^{-1}). At this stage straining is confined essentially to a single conjugate pair. Notice irregular margins of ductile fractures and variations in their trends.

[1]GSA Data Repository item 2010092, Figure DR1 (reconstruction of country rock blocks separated by magma intrusion) and Figure DR2 (stereonet plots of dike attitudes and dike intersection orientations), is available online at www.geosociety.org/pubs/ft2010.htm, or on request from editing@geosociety.org or Documents Secretary, GSA, P.O. Box 9140, Boulder, CO 80301, USA.

gradients (Shigematsu et al., 2004). Fast deviatoric stress relaxation in weak (hot) rocks will have a similar effect.

Void nucleation by shear displacement gives rise to ductile fracture sets, initially at 90°, following the maximum shear stress trajectories. However, straining due to ductile fracturing causes volume increases due to ductile dilatant behavior. As the void volume increases, the orientations of the two shear planes rotate and approach each other, becoming nearly parallel in extreme cases. In this case, ductile fracture dikes assume the direction of a brittle-elastic dike, with the difference of having accomplished a net elliptical expansion rather than a net uniaxial expansion.

Additional deviation in orientation occurs during fracture growth because of stress perturbations at fracture tips, and interaction with other cracks or strength heterogeneities. As the fracture network matures, blocks may rotate, changing preexisting fractures, and modifying the stress tensor controlling further fracture growth. These effects may explain the variety of orientations and their tortuosity in the numerical models (Fig. 3A). In nature, external stress fluctuation, and the presence of magmas (Fig. 2), might further accentuate these variations, leading to complex networks.

Results here are valid for ductile fracturing in solid rocks with access to an external fluid or melt source, or low fluid-filled or melt-filled porosity (<7%) (Rosenberg and Handy, 2005). They are likely also valid for rocks with higher melt fractions, provided the stress-bearing solid framework is not disrupted. The results are limited to pure shear systems. Thus, diking by ductile fracturing provides a mechanism for melt extraction from rocks with low melt fraction, avoiding problems of initiating and propagating brittle-elastic dikes through low-viscosity rocks. We postulate that catastrophic ductile failure at stage 3 could give rise to a dike with sufficient buoyancy to overcome fracture toughness at its tip, or it could allow magma to migrate into colder or more competent regions where brittle-elastic diking takes over. Thus, ductile fracture dikes may be the progenitors of brittle-elastic dikes.

We conclude that ductile fracturing drives magma migration in deforming hot, deep systems, and it explains a number of natural features. Ductile fracturing could also solve one of the major riddles surrounding new plate generation at mid-ocean ridges, by providing an alternative mechanism for formation of fast melt-extraction channel ways, which have been postulated as the general means of melt extraction at mid-ocean ridges (Stracke et al., 2006).

ACKNOWLEDGMENTS

We thank G. Solar, S. Cruden, C. Meriaux, H. Sheldon, P. Bons, and P. Eichhubl for careful, helpful, and constructive comments on earlier versions of the manuscript.

REFERENCES CITED

Bons, P.D., and van Milligen, B.P., 2001, A new experiment to model self-organized critical transport and accumulation of melt and hydrocarbons from their source rocks: Geology, v. 29, p. 919–922, doi: 10.1130/0091-7613(2001)029<0919:NETMSO>2.0.CO;2.

Brown, M., 2004, The mechanisms of melt extraction from lower continental crust of orogens: Is it a self-organized critical phenomenon?: Transactions of the Royal Society of Edinburgh, Earth Sciences, v. 95, p. 35–48, doi: 10.1017/S0263593300000900.

Chen, Z., and Jin, Z.-H., 2006, Magma-driven subcritical crack growth and implications for dike initiation from a magma chamber: Geophysical Research Letters, v. 33, p. doi: 10.1029/2006Gl026979.

Connolly, J.A.D., and Podladchikov, Y.Y., 1998, Compaction-driven fluid flow in viscoelastic rock: Geodinamica Acta, v. 11, p. 55–84.

Dimanov, A., Rybacki, E., Wirth, R., and Dresen, G., 2007, Creep and strain-dependent microstructures of synthetic anorthite-diopside aggregates: Journal of Structural Geology, v. 29, p. 1049–1069, doi: 10.1016/j.jsg.2007.02.010.

Eichhubl, P., 2004, Growth of ductile opening-mode fractures in geomaterials, *in* Cosgrove, J.W. and Engelder, T., eds, The Initiation, Propagation, and Arrest of Joints and Other Fractures: Geological Society of London Special Publication 231, p. 11–24.

Eichhubl, P., and Aydin, A., 2003, Ductile opening-mode fracture by pore growth and coalescence during combustion alteration of siliceous mudstone: Journal of Structural Geology, v. 25, p. 121–134, doi: 10.1016/S0191-8141(02)00055-X.

Gandhi, C., and Ashby, M.F., 1979, Fracture-mechanism maps for materials which cleave: F.C.C., B.C.C. and H.C.P. metals and ceramics: Acta Metallurgica, v. 27, p. 1565–1602, doi: 10.1016/0001-6160(79)90042-7.

Hirth, G., and Tullis, J., 1994, The brittle-plastic transition in experimentally deformed quartz aggregates: Journal of Geophysical Research, v. 99, p. 11,731–11,747, doi: 10.1029/93JB02873.

Hirth, G., Teyssier, C., and Dunlap, W.J., 2001, An evaluation of quartzite flow laws based on comparisons between experimentally and naturally deformed rocks: International Journal of Earth Sciences, v. 90, p. 77–87, doi: 10.1007/s005310000152.

Knott, J.F., 1973, Fundamentals of Fracture Mechanics: London, The Pitman Press, 273 p.

Lister, J.R., and Kerr, R.C., 1991, Fluid-mechanical models of crack propagation and their application to magma transport in dykes: Journal of Geophysical Research, v. 96, p. 10,049–10,077, doi: 10.1029/91JB00600.

Needleman, A., and Tvergaard, V., 1992, Analyses of plastic flow deformation in metals: Applied Mechanics Reviews, v. 45, p. 3–18, doi: 10.1115/1.3121390.

Petford, N., and Koenders, M.A., 1998, Self-organization and fracture connectivity in rapidly heated continental crust: Journal of Structural Geology, v. 20, p. 1425–1434, doi: 10.1016/S0191-8141(98)00081-9.

Petford, N., Cruden, A.R., McCaffrey, K.J.W., and Vigneresse, J.-L., 2000, Granite magma formation, transport and emplacement in the Earth's crust: Nature, v. 408, p. 669–673, doi: 10.1038/35047000.

Pollard, D.D., and Segall, P., 1987, Theoretical displacement and stresses near fractures in rock: With application to faults, joints, veins, dikes and solution surfaces, *in* Atkinson, B.K., ed., Fracture Mechanics in Rocks: New York, Elsevier, p. 277–349.

Regenauer-Lieb, K., 1999, Dilatant plasticity applied to Alpine collision: Ductile void growth in the intraplate area beneath the Eifel volcanic field: Journal of Geodynamics, v. 27, p. 1–21, doi: 10.1016/S0264-3707(97)00024-0.

Rogers, H.C., 1979, Adiabatic plastic deformation: Annual Review of Materials Science, v. 9, p. 283–311, doi: 10.1146/annurev.ms.09.080179.001435.

Rolland, Y., and Pêcher, A., 2001, The Pangong granulites of the Karakoram fault (western Tibet): Vertical extrusion within a lithosphere-scale fault?: Comptes Rendus de L'Academie des Sciences, Serie II, Fascicule A–Sciences de la Terre et des Planetes, v. 332, p. 363–370.

Rosenberg, C.L., and Handy, M.R., 2005, Experimental deformation of partially melted granite revisited: Implications for the continental crust: Journal of Metamorphic Geology, v. 23, p. 19–28, doi: 10.1111/j.1525-1314.2005.00555.x.

Rubin, A.M., 1998, Dike ascent in partially molten rock: Journal of Geophysical Research, v. 103, p. 20,901–20,919, doi: 10.1029/98JB01349.

Rubin, K.H., Van Der Zander, I., Smith, M.C., and Bergmanis, E.C., 2005, Minimum speed limit for ocean ridge magmatism from ^{210}Pb-^{226}Ra-^{230}Th disequilibria: Nature, v. 437, p. 534–538, doi: 10.1038/nature03993.

Rushmer, T., 1995, An experimental deformation study of partially molten amphibolite: Application to low-melt fraction segregation: Journal of Geophysical Research, v. 100, p. 15,681–15,695, doi: 10.1029/95JB00077.

Rybacki, E., Wirth, R., and Dresen, G., 2008, High-strain creep of feldspar rocks: Implications for cavitation and ductile fracture in the lower crust: Geophysical Research Letters, v. 35, p. L04304, doi: 10.1029/2007GL032478.

Shigematsu, N., Fujimoto, K., Ohtani, T., and Goto, K., 2004, Ductile fracture of fine-grained plagioclase in the brittle-plastic transition regime: Implication for earthquake source nucleation: Earth and Planetary Science Letters, v. 222, p. 1007–1022, doi: 10.1016/j.epsl.2004.04.001.

Stockhert, B., Brix, M.R., Kleinschrodt, R., Hurford, A.J., and Wirth, R., 1999, Thermochronometry and microstructures of quartz—A comparison with experimental flow laws and predictions on the temperature of the brittle-plastic transition: Journal of Structural Geology, v. 21, p. 351–369, doi: 10.1016/S0191-8141(98)00114-X.

Stracke, A., Bourdon, B., and McKenzie, D., 2006, Melt extraction in the Earth's mantle: Constraints from U-Th-Pa-Ra studies in oceanic basalts: Earth and Planetary Science Letters, v. 244, p. 97–112, doi: 10.1016/j.epsl.2006.01.057.

Thomason, P.F., 1989, Ductile Fracture of Metals: Oxford, UK, Pergamon Press, 219 p.

Tvergaard, V., and Needleman, A., 1992, Elastic-viscoplastic analysis of ductile failure, *in* Besdo, D., and Stein, E., eds., Finite Inelastic Deformation Theory and Applications: Berlin, Springer-Verlag, p. 3–14.

Weinberg, R.F., 1999, Mesoscale pervasive melt migration: Alternative to dyking: Lithos, v. 46, p. 393–410, doi: 10.1016/S0024-4937(98)00075-9.

Weinberg, R.F., and Mark, G., 2008, Magma migration, folding, and disaggregation of migmatites in the Karakoram shear zone, Ladakh, NW India: Geological Society of America Bulletin, v. 120, p. 994–1009, doi: 10.1130/B26227.1.

Weinberg, R.F., and Podladchikov, Y., 1994, Diapiric ascent of magmas through power-law crust and mantle: Journal of Geophysical Research, v. 99, p. 9543–9559, doi: 10.1029/93JB03461.

Závada, P., Schulmann, K., Konopásek, J., Ulrich, S., and Lexa, O., 2007, Extreme ductility of feldspar aggregates—Melt-enhanced grain boundary sliding and creep failure: Rheological implications for felsic lower crust: Journal of Geophysical Research–Solid Earth, v. 112, p. B10210, doi: 10.1029/2006JB004820.

Manuscript received 22 June 2009
Revised manuscript received 2 November 2009
Manuscript accepted 9 November 2009

Printed in USA